Aron Phoebe, G (Orcid ID: 0000-0002-4700-5445)
Poulsen Christopher James (Orcid ID: 0000-0001-5104-4271)
Fiorella Richard P (Orcid ID: 0000-0002-0824-4777)
Matheny Ashley M (Orcid ID: 0000-0002-9532-7131)

Stable Water Isotopes Reveal Effects of Intermediate Disturbance and Canopy Structure on Forest Water Cycling

Phoebe G. Aron[1], Christopher J. Poulsen[1], Richard P. Fiorella[2], and Ashley M. Matheny[3]

[1]Department of Earth and Environmental Sciences, University of Michigan, Ann Arbor, MI 48109, USA. [2]Department of Geology and Geophysics, University of Utah, Salt Lake City, UT 84112, USA. [3] Department of Geological Sciences, Jackson School of Geosciences, University of Texas, Austin, TX 78712, USA.

Corresponding author: Phoebe Aron (paron@umich.edu)

Key Points:

- Intermediate disturbance can change the contribution of entrained, evaporated, and transpired water vapor to forest canopies

- Canopy gaps increase hydrologic mixing between the surface layer and the free atmosphere

- The assumption of a well-mixed canopy-atmosphere may be violated in the case of thick, homogeneous forest canopies

Abstract

Forests play an integral role in the terrestrial water cycle and link exchanges of water between the land surface and the atmosphere. To examine the effects of an intermediate disturbance on forest water cycling, we compared vertical profiles of stable water vapor isotopes in two closely located forest sites in northern lower Michigan. At one site, all canopy-dominant early successional species were stem-girdled to induce mortality and accelerate senescence. At both sites, we measured the isotopic composition of atmospheric water vapor at six heights during three seasons (spring, summer, and fall), and paired vertical isotope profiles with local meteorology and sap flux. Disturbance had a substantial impact on local water cycling. The undisturbed canopy was moister, retained more transpired vapor, and at times was poorly mixed with the free atmosphere above the canopy. Differences between the disturbed and undisturbed sites were most pronounced in the summer when transpiration was high. Differences in forest structure at the two sites also led to more isotopically stratified vapor within the undisturbed canopy. Our findings suggest that intermediate disturbance may increase mixing between the surface layer and above-canopy atmosphere and alter ecosystem-atmosphere gas exchange.

Keywords: water cycle, stable water isotopes, intermediate disturbance, canopy structure, evapotranspiration

Plain Language Summary

Forests play an important role in the climate system and link water fluxes between the land surface and the atmosphere. Here we compare water vapor isotopes in two adjacent forest sites in the northern lower peninsula of Michigan to understand the effects of intermediate disturbance and canopy structure on forest water cycling. One site is dominated by aspen and birch and has a thick, closed canopy. All of the aspen and birch were killed at the second site. As a result, the disturbed site has a more open canopy structure. From our comparison, we found that both the species of tree and the spacing around trees are important controls on forest water cycling. With more space between trees, air mixes more freely into the canopy, which dries the forest air. Alternatively, air may be poorly mixed within and above thick, closed canopies.

1 Introduction

Forests cover one-third of Earth's surface and play important roles regulating carbon storage, freshwater, and climate (FAO, 2015). As part of the terrestrial water cycle, forests promote rainfall, cool surface temperatures, transport water across vast landscapes, and regulate water supplies (Ellison et al., 2017). Globally, vegetation recycles a tremendous amount of water to the atmosphere via transpiration; forests account for approximately 50% of this flux (Schlesinger & Jasechko, 2014; Xiao, Wei, & Wen, 2018). However, as the frequency of environmental disturbances from natural and anthropogenic forces accelerate, forest hydrological cycles may change (Ellison et al., 2017; Pan et al., 2011). Accordingly, changes in forest cover may affect rainfall and water availability, water transport, and local and global temperatures

2

(Debortoli et al., 2017; Ellison et al., 2017; Hesslerová, Pokorný, Brom, & Rejšková-Procházková, 2013; Jasechko et al., 2013). Understanding the links between forest structure and water cycling is necessary to better predict future temperature and precipitation patterns and to manage freshwater resources.

Forest disturbances range from complete stand-clearing events to subtle changes that target select species or affect the canopy irregularly. Intermediate disturbances, which do not trigger complete stand replacement, occur naturally though pest infestations (Herms & McCullough, 2014; Logan, Régnière, & Powell, 2003), ecological succession (Gough et al., 2013; Hardiman, Bohrer, Gough, & Curtis, 2013), or extreme weather events such as fire, ice storms, strong winds, or drought (Anderegg et al., 2018; He & Mladenoff, 1999; Mcdowell et al., 2008; Mitchell, 2013; Trugman, Medvigy, Anderegg, & Pacala, 2018). Intermediate disturbances can also be anthropogenically driven by selective logging (Asase, Asiatokor, & Ofori-Frimpong, 2014; Asner, Keller, Pereira, Zweede, & Silva, 2004), prescribed fire management (Parsons & DeBenedetti, 1979; Stephens et al., 2009), arson or accidental human fire ignition (Ganteaume et al., 2013), or human land use (Schulte, Mladenoff, Crow, Merrick, & Cleland, 2007). Each of these mechanisms alters forest canopy function through changes in the vertical distribution of solar radiation (Hardiman et al., 2013), soil moisture (He et al., 2013), evapotranspiration partitioning (Matheny et al., 2014), air temperature, humidity, wind speed, and turbulent mixing (Maurer, Hardiman, Vogel, & Bohrer, 2013), and thus affect the microclimate and water cycle within the canopy (Baldocchi, Wilson, & Gu, 2002; Chen et al., 1999).

Forest structure and water cycling are linked through exchanges of mass and energy. Photosynthesis, transpiration, respiration, and stomatal conductance depend on temperature, relative humidity, and light. The physical arrangement of trees in a forest creates drag and turbulence (Maurer et al., 2013), intercepts and scatters light (Atkins, Fahey, Hardiman, & Gough, 2018; Hardiman et al., 2018), and modulates heat received by soil and leaves (Baldocchi & Meyers, 1998). In turn, energy evaporates water, either from the soil or through transpiration, and generates sensible heat. Although forests are susceptible to an array of intermediate disturbances, potential changes of mass and energy exchanges following changes to canopy structure are not completely understood. Here, we use stable water isotopes to study water cycling at two forest sites, one disturbed and one undisturbed, and examine the effects of an intermediate disturbance on canopy moisture and forest water cycling.

Stable water isotopes are tracers of hydrologic processes and may be used to better understand ecosystem-atmosphere water exchange. Phase changes of water preferentially partition heavy isotopologues into the liquid or solid phase while light isotopologues remain in the higher energy vapor phase (Gat, 1996). At equilibrium, this fractionation is temperature dependent (Horita & Wesolowski, 1994). When the two phases are not in equilibrium, an additional kinetic fractionation arises due to differences in the diffusivities among isotopologues. The difference in diffusivity between $H_2^{18}O/H_2^{16}O$ is larger than that for $HDO/{}^1H_2O$, which results in a stronger kinetic effect on oxygen isotopes than hydrogen isotopes (Cappa, 2003; Luz, Barkan, Yam, & Shemesh, 2009; Merlivat, 1978). The degree of kinetic fractionation is often

3

quantified using deuterium excess ($d = \delta D - 8*\delta^{18}O$ (Dansgaard, 1964)), which is a measure of deviation from the global meteoric water line (GMWL, $\delta D = 8*\delta^{18}O + 10‰$ (Craig, 1961)).

Advances in laser-based, high-resolution, near-continuous water isotope analyzers have revolutionized water vapor isotope monitoring and greatly broadened the scales of hydrologic spatiotemporal variability that can be studied. At the boundary layer and surface level, isotope ratios of water vapor have been measured to investigate moisture sources (Delattre, Vallet-Coulomb, & Sonzogni, 2015; Fiorella, Poulsen, & Matheny, 2018; Galewsky & Samuels-Crow, 2015; Noone et al., 2013; Steen-Larsen et al., 2015), quantify entrainment and evapotranspiration (ET) (He & Smith, 1999; Huang & Wen, 2014; Lai & Ehleringer, 2011; Simonin et al., 2014; Welp et al., 2012), and partition the ET flux (Aemisegger et al., 2014; Good et al., 2014; Xiao et al., 2018). Together, this work demonstrates the utility of water vapor isotope measurements as a tool to study water fluxes between ecosystems and the atmosphere. The high temporal resolution of vapor isotope measurements from laser-based analyzers captures rapid, sub-diurnal (minutes to hours) changes in water cycling and links surface hydrology with biotic cycles and atmospheric conditions.

Isotope ratios of water vapor can expand our current understanding of forest hydrology because the fluxes and processes that act to dry or moisten canopies – entrainment, evaporation, and transpiration – have distinct isotopic signatures. During clear conditions, entrainment tends to dry canopy air with vapor that is isotopically more depleted than air within the canopy (Welp et al., 2012). Evaporation moistens canopy air with vapor that is relatively depleted in heavy isotopes and has a high d due to the high degree of kinetic fractionation associated with the phase change from soil water to water vapor (Barnes & Allison, 1984). The isotopic signature of transpiration is more complicated and depends on timescale, vegetation type, and microclimates within the canopy. Over timescales greater than leaf-water turnover times, the isotopic composition of transpired vapor must equal that of source water taken up at the roots since plants generally do not fractionate soil water during root uptake (Ehleringer & Dawson, 1992). However, on shorter timescales, the isotopic composition of transpired vapor may deviate from source water (Cernusak, Pate, & Farquhar, 2002; Harwood, Gillon, Griffiths, & Broadmeadow, 1998; Simonin et al., 2013; Welp et al., 2008).

In this study, we measured vertical profiles of water vapor isotopes in two closely located forest sites in northern Michigan. The control site is representative of forests in the northern Great Lakes region; at the experimental site, an intermediate disturbance was prescribed to test the effects of this disturbance on forest processes. Our objectives were to: 1) quantify the temporal variation of vapor $\delta^{18}O$ and δD at the two sites, 2) use the isotopic composition of water vapor to compare water cycling at disturbed and undisturbed sites, and 3) identify patterns and controls on canopy moisture. The sites in this study are hydrologically and meteorologically well studied (e.g. He et al., 2013; Matheny et al., 2014; Maurer et al., 2013). Therefore, an additional goal is to explore how vapor isotope profiles and flux tower measurements complement each other or provide similar information about water cycling. This goal may inform future vapor isotope studies that are not collocated with flux towers or sap flux networks.

The addition of isotope measurements at these field sites improves our understanding of forest hydrologic responses to intermediate disturbance and expands the use of water vapor isotopes to study land-atmosphere interactions.

2 Materials and Methods

2.1 Site Description

This study was conducted at two field sites at the University of Michigan Biological Station (UMBS) in northern lower Michigan, USA. Mean annual temperature at UMBS is 6.8°C and the site receives an average 805 mm of precipitation annually (Matheny et al., 2014). Soils are well drained Haplorthods of the Rubicon, Blue Lake, or Cheboygan series and consist of 92.2% sand, 6.5% silt, and 0.6% clay (Nave et al., 2011). Water isotope measurements were conducted at two adjacent UMBS sites (~1.2 km apart) with collocated eddy covariance towers. Both flux towers are affiliated with the AmeriFlux network (http://ameriflux.lbl.gov/).

The forest surrounding the control site (45°35'35" N, 84°41'48" W, AmeriFlux database site-ID US-UMB), hereafter referred to as the undisturbed site, is dominated by early successional bigtooth aspen (*Populus grandidentata*) and paper birch (*Betula papyrifera*), but is transitioning to a mixed composition of mid-successional red oak (*Quercus rubra*), red maple (*Acer rubrum*), white pine (*Piuns strobus*), American beech (*Fagus grandifolia*), and sugar maple (*Acer saccharum*). The tight arrangement of trees and closed, broadleaf canopy cover at this site is representative of many forests in the northern Great Lakes region. This site has remained undisturbed since the region was extensively logged in the early twentieth century. The tower at the disturbed site (45°33'45" N, 84°41'51" W, AmeriFlux database site-ID US-UMd) is located within the Forest Accelerated Succession ExperimenT (FASET) plot, hereafter referred to as the disturbed site. In 2008, all aspen and birch in a 39 ha stand around the disturbed site's tower were stem girdled to induce mortality of early successional species and evaluate the effects of ecologic succession. Additional information about the FASET experiment and site details are available in Gough et al. (2013).

Prior to the disturbance, forest composition, structure, and meteorological conditions were similar at the undisturbed and disturbed sites. Persistent differences in forest structure and water cycling (He et al., 2013; Matheny et al., 2014) have developed since the disturbance as a result of a younger, more open, structurally complex canopy at the disturbed site (Hardiman et al., 2013; Maurer et al., 2013). As a result of the girdling treatment, the disturbed canopy has more deep gaps and clumped vegetation than the undisturbed canopy.

2.2 Water Vapor Isotope Measurements

We deployed cavity ring-down spectrometers (CRDS) in temperature-controlled sheds near both eddy covariance towers. At the undisturbed site, a Picarro L2120-i was installed on April 16, 2016. A Picarro L2130-i was installed at the disturbed site on April 25, 2016. Both analyzers were removed on October 1, 2016. Two liquid internal laboratory standards (-8.33‰

5

and -55.86‰ (heavy standard) and -23.81‰ and -181.35‰ (light standard) for $\delta^{18}O$ and δD, respectively) were measured approximately every 12 hours to monitor for drift and calibrate isotope data to the VSMOW–SLAP scale (Bailey, Noone, Berkelhammer, Steen-Larsen, & Sato, 2015). Standards were introduced as a continuous stream using a Standard Delivery Module (SDM) and high precision vaporizer (A0110) maintained at 140°C and ambient pressure. A Drierite (26800) column was used to dry ambient air for standards analysis. Laboratory standards were measured at water vapor concentrations between 10,000 and 30,000 ppmv.

We used version 1.2 of the University of Utah vapor processing scripts (Fiorella, Bares, Lin, Ehleringer, & Bowen, 2018) to calibrate ~1 Hz isotope data and determine instrument precision. We found that isotope values varied with humidity. As a result, we varied the SDM delivery rate of liquid standards and measured isotopic compositions from 2,000 to 30,000 ppm to develop equations and correct for this apparent humidity bias. We measured both internal standards at each injection rate for 20 minutes, but only analyzed measurements from the last 10 minutes of each humidity level to avoid memory effects between different standards or injection rates. Within a humidity range (here 15,000-25,000 ppm) where the response between cavity humidity and isotopic composition was minimal, we calculated the deviation of measured isotopic compositions from the true isotopic composition. We then developed and applied correction equations, determined by a linear regression of the deviation between measured and true isotopic compositions against the inverse of cavity humidity within the 15,000-25,000 ppm range, to correct isotope data for the dependence on cavity humidity. Additional details on this cavity humidity correction are provided in the Supplementary materials. Instrument precision also depended on cavity humidity. We present the 1σ uncertainty at 5,000 ppmv, the lowest measured vapor mixing ratio during our sampling campaign, and 15,000 ppmv, near the average mixing ratio across all three sampling periods. For d, we assume oxygen and hydrogen errors are independent. At the undisturbed site, 1σ uncertainty ranged from 0.43‰ for $\delta^{18}O$, 1.51‰ for δD, and 3.73‰ for d at 5,000 ppmv to 0.24‰, 0.74‰, and 2.02‰ (for oxygen, hydrogen, and d, respectively) at 15,000 ppm. At the disturbed site, 1σ uncertainty ranged from 0.20‰, 0.68‰, and 1.73‰ at 5,000 ppmv to 0.11‰, 0.35‰, and 0.94‰ (oxygen, hydrogen, and d, respectively) at 15,000 ppm.

Each eddy covariance tower was equipped with a vapor sampling manifold that included intake lines at five heights within the canopy and one above the canopy. Within-canopy vapor was sampled at 2, 5, 10, 15, and 20 m above the forest floor. Above-canopy vapor was sampled at 32 m (disturbed site) and 34 m (undisturbed site). The above-canopy sampling port was collocated with meteorological and flux measurements from the towers. A diaphragm pump operated at ~5 L/min on each sampling manifold to ensure continual airflow and minimize memory effects between samples. Sampling lines were constructed with Bev-A-Line tubing to prevent fractionation (Simonin et al., 2013), encased in insulation, and wrapped with a warm wire to prevent condensation.

Each CRDS was setup to control a multi-position valve (VICI/Valco EMT2SD6MWE) to switch between sampling heights. Each port was measured for 5 minutes; we omit the first 2

minutes of each measurement to account for memory effects from switching positions and used the mean of the last 3 minutes of each measurement for analysis (Aemisegger et al., 2012). We measured 48 vertical profiles of vapor isotopes each day. Within each profile, the 3-minute average of isotopic measurements from each sampling port is assumed to represent the isotopic composition at that height for the full 30-minute profile.

We focus on three time periods during the 2016 growing season: May 10-31 (spring, DOY 131-151), June 7-30 (summer, DOY 159-182), and September 21-30 (fall, DOY 265-274). For convenience we refer to the three time periods as spring, summer, and fall, respectively. We do not include winter measurements because we expect canopy structure to have little effect on water fluxes when trees are bare and dormant. Missing records are due to equipment malfunction and electrical problems at the field sites. In August 2016, the analyzer from the disturbed site was temporarily moved to a different location for another study.

2.3 Meteorological, Sap Flux, and Eddy Covariance Measurements

Temperature and relative humidity (HMP45g, Vaisala, Helsinki, Finland) were measured at 2 m and above the canopy at 32 or 34 m (disturbed and undisturbed sites, respectively) at each site. The 2 m meteorological towers were located approximately 60 m from each flux tower. Temperature and relative humidity sensors were removed from the disturbed site in the late summer. Replacement equipment was installed 1 m above the forest floor near the disturbed site flux tower, but only recorded temperature. Surface pressure (PTB101B, Vaisala, Helsinki Finland) was measured at ground level at the undisturbed site. Sap flux, which was measured as a proxy for transpiration, was continuously measured in 60 trees at each site with Granier-style (Granier, 1987) thermal dissipation probes. Additional details about sap flux measurements at UMBS are available in Matheny et al. (2014). Eddy covariance CO_2 and H_2O fluxes were measured above the canopies at 32 and 34 m. The latent heat flux was measured at high resolution (10 Hz) using the eddy covariance approach: water vapor and CO_2 concentrations were measured using closed-path infrared gas analyzers (LI7000, LI-COR Biosciences, Lincoln, NE, USA); wind velocity and temperature were measured with a 3-D ultrasonic anemometer (CSAT3, Campbell Scientific, Logan, UT, USA). Details about eddy flux data processing are available in Gough et al. (2013) and Matheny et al. (2014). Above-canopy variables and 1 m temperature measurements were reported as 30-minute averages. Sap flux and 2 m meteorological measurements were collected every minute and averaged to 30-minute time steps to facilitate analysis with isotopic measurements. Daily precipitation amount was measured approximately 4 miles east of UMBS at the Pellston Regional Airport and accessed from the NOAA Climate Data Online archive (Network ID USW00014841).

7

3 Results

3.1 Seasonal Variability

All δ^{18}O and δD vapor values are plotted in Figure 1. Isotopic compositions cluster around the GMWL during all three seasons with a consistent, slightly shallower slope than the global meteoric water line. In general, isotopic trends were similar for oxygen and hydrogen; therefore, we show and discuss only δ^{18}O throughout this section.

On timescales longer than a day, isotopic and meteorologic trends were similar at the disturbed and undisturbed sites (Figures 2 and S11-S12). Seasonal comparisons between the two sites were generally consistent across the spring, summer, and fall measurement periods, so we focus primarily on summer conditions and include additional information about spring and fall conditions in the Supplement. Vapor δ^{18}O varied between -14 and -26‰ at both sites and was typically greater at the surface and lower in the upper canopy (10-20 m) (Figures 2 and S11-S12 a and i). On average, vapor δ^{18}O, specific humidity (q), temperature, and vapor pressure deficit (VPD) were highest in the summer and lower in the spring and fall (Figures 2 and S11-S12 a,c,d,e and i,k,l,m). Sap flux increased through the spring sampling period, was at a maximum in the summer, and was at a minimum in the fall (Figures 2 and S11-S12 g and o). The seasonal magnitudes of sap flux are consistent with leaf area index (LAI) trends as canopies at both sites leafed out during the spring sampling period, were at their maximum extent during the summer, and were in decline in the fall. Wind speed did not vary on seasonal timescales, but rather, associated with the passing of synoptic scale weather systems, meandered on a 2-4 day timescale with very few excursions beyond a small range (1-5 m/s) (Figures 2 and S11-S12 f and n).

Despite the general coherence between isotopes, meteorology, and ecohydrology on seasonal timescales at UMBS, differences emerged between the disturbed and undisturbed sites (Figure 3, Table 1). During the spring and summer, vapor at the disturbed site was generally more depleted in heavy isotopes than at the undisturbed site (Figures 3a and 3i). This difference was more pronounced in the summer (1-2‰ difference) than in the spring (~ 0.4‰). Within the canopies, mean spring and summer d was ~ 0.3‰ greater at the undisturbed site (Figures 3b and 3j). Although the magnitude of between-site d differences was greater in the summer than in the spring, this difference is not statistically significant. In the fall, the disturbed site was generally more depleted in heavy isotopes than the undisturbed site (Figure 3q) and d was 4-8‰ greater at the undisturbed site (Figure 3r). In all three seasons the disturbed site was drier than the undisturbed site (Figures 3c, 3k, and 3s). Above the canopy, air temperature was ~0.4 °C warmer at the undisturbed site (Figures 3d, 3l, and 3t) while VPD was nearly identical (< 0.04 kPa difference, Figures 3e, 3m, and 3u). Near the surface (2 m), air temperature was ~0.6 °C cooler (Figures 3d, 3l, and 3t) and VPD ~0.15 kPa lower at the undisturbed site (Figures 3e, 3m, and 3u). Mean wind speed was ~1 m/s greater at the undisturbed site than the disturbed site (Figures 3f, 3n, and 3v), and sap flux was almost always greater at the undisturbed site than the disturbed site (Figures 3g, 3o, and 3w). Mean seasonal differences of isotopes, meteorology, and sap flux

8

are presented in Table 1 with significant differences ($p < 0.05$) between the disturbed and undisturbed sites highlighted.

The two sites also exhibited isotopic differences with height. While $\delta^{18}O$ was generally greater near the surface than in the upper canopy, vertical gradients of $\delta^{18}O$ within the canopies were larger at the undisturbed site than at the disturbed site (Figure 4). Summer and fall $\delta^{18}O$ gradients within the undisturbed canopy (2 – 20 m) were pronounced at night (0.70‰ and 0.95‰ in the summer and fall, respectively) but dissipated through the day (Figure 4 a-d). The disturbed site did not exhibit the same stratified nighttime isotopic compositions and was relatively well mixed with vertical gradients generally less than 0.25‰ (Figure 4 e-h). Within each season, q ratios exhibited little variation at any of the sampling heights (Figure S13).

3.2 Synoptic Variability

Passing weather systems drove relatively large shifts of isotopes, meteorology, and sap flux within a few days. We focus on a summer storm (DOY 166-171) and examine how isotopes, sap flux, and eddy covariance data reveal information about the hydrologic fluxes associated with this event. 0.69 mm of rain fell on DOY 167. We include one day of pre-storm conditions (DOY 166) and define the end of the storm as the day during which VPD at the undisturbed site was at a maximum following the rainfall event. We calculated the isotopic composition of the ET flux ($\delta^{18}O_{ET}$) at 20 m with a Keeling mixing model (Keeling, 1958; Yakir & Sternberg, 2000), and followed the methods described by Williams et al. (2004) to partition the transpiration component of ET (defined here as T/ET) from sap flux and eddy covariance measurements.

Prior to the storm, conditions at the disturbed and undisturbed site were similar but reflect the consistent seasonal differences at the two sites: sap flux was greater, $\delta^{18}O$ higher, and air moister at the undisturbed site than at the disturbed site (Figure 5). Transpiration accounted for a greater proportion of the ET flux at the undisturbed site (~ 70%) than the disturbed site (~ 50%) (Figure 5b). Rain fell from 10:00 to 17:00 on DOY 167. During the event, sap flux and VPD decreased to nearly zero while q and $\delta^{18}O$ increased (Figure 6). Immediately after the storm (DOY 168) increases in VPD, sap flux, and T/ET drove $\delta^{18}O_{ET}$ and $\delta^{18}O$ of ambient vapor to higher values. By DOY 169 and 170, sap flux and VPD returned to pre-storm values and were similar at the disturbed and undisturbed sites (Figure 5 c-d and g-h). At the same time, isotopic differences emerged at the two sites (Figure 5a Figures 6 a-b and e-f).

3.3 Diurnal Cycles

Vapor $\delta^{18}O$ and d generated clear diurnal cycles at both the disturbed and undisturbed sites (Figure 7). Diurnal cycles emerged in the spring, were most pronounced during the summer, and decreased in amplitude in the fall. Generally, $\delta^{18}O$ increased slightly just after sunrise to an early-morning peak, decreased through the day to a late afternoon minimum, and increased in the early evening before sunset (Figure 7, top row). Nighttime $\delta^{18}O$ values exhibited little variation. The diurnal d cycle was apparent in all three seasons and at both sites (Figure 7, second row). d

9

was relatively constant at night, decreased briefly just after sunrise, increased in the morning to a mid-day maximum, and decreased rapidly in the late afternoon. In all three seasons, the timing of the diurnal *d* cycle was consistent between sites but the amplitude and rate of change differed. *q* exhibited very little diurnal variation (Figure 7, third row).

Diurnal temperature generally peaked in the mid-afternoon and was at a minimum just before sunrise (Figure 7, fourth row); relative humidity exhibited the opposite diurnal cycle with the greatest values just before sunrise and the lowest values in the mid-afternoon (Figure 7, fifth row). Like temperature, diurnal vapor pressure deficit (VPD) increased in the morning and decreased in the afternoon (Figure 7, sixth row). In the spring and summer, diurnal wind speed exhibited a distinct cycle with maximum values in the mid-afternoon and minimum values around sunrise. There was no clear diurnal cycle of wind speed in the fall at either site (Figure 7, seventh row). At both sites, sap flux began at sunrise, reached a maximum in the early afternoon, and was nearly zero by sunset (Figure 7, eighth row). The shape of the diurnal sap flux cycle was consistent throughout all three seasons, but the maximum summer diurnal sap flux was approximately two times greater than sap flux in the spring or fall periods (Figure 7, eighth row).

Isotopic, meteorologic, and sap flux differences also emerged at the disturbed and undisturbed sites on diurnal timescales. In the summer and fall, the early morning $\delta^{18}O$ peak was more pronounced at the undisturbed site than at the disturbed site (Figure 7 q,ag and y,ao). In addition, although the magnitude of diurnal *d* cycles was similar at the two sites (~12, 20, and 8 ‰ in the spring, summer, and fall, respectively), daytime patterns differed (Figure 7, second row). In all three seasons, *d* increased rapidly in the undisturbed canopy in the early morning and maintained a high plateau through the day. In contrast, at the disturbed site, *d* increased gradually through the early morning and mid-afternoon and peaked in the late afternoon. Vertical gradients of meteorological conditions between the surface and 32/34 m were greater at the undisturbed site than the disturbed site (Figure 7, fourth and fifth rows). Similarly, diurnal wind speed and sap flux were greater at the undisturbed site than the disturbed site (Figure 7, rows seven and eight, respectively).

4 Discussion

4.1 Seasonal Variability

Observed seasonal isotopic shifts reflect changes in large-scale circulation and seasonal wind patterns, which we expect to be similar at the disturbed and undisturbed sites (Gat, Bowser, & Kendall, 1994). In northern Michigan, air advected from the north is drier and has experienced colder temperatures along its trajectory than air from the south (Rasmusson, 1968). As a result, at UMBS the boundary layer was cooler, drier, and more depleted in heavy isotopes in the spring and fall than was observed in the summer. Sap flux trends point to seasonal variability of transpiration at UMBS (Figures 2 and S11-S12 g and o). Sap flux increased through the spring as the canopies leafed out and hydrologic cycling intensified during the beginning of the growing

season, was greatest during the summer when the canopies were fully developed, and was low in the fall when transpiration was in decline at the end of the growing season.

Seasonal $\delta^{18}O$ differences between the disturbed and undisturbed site may be explained by canopy structure, the magnitude of local water fluxes, and different species-specific ecohydrological strategies that have previously been observed at UMBS (Matheny et al., 2014, 2016; Thomsen et al., 2013). The 2008 girdling treatment altered the spatial arrangement of vegetation and increased gaps between trees at the disturbed site. As a result, light reaches deeper (Hardiman et al., 2013), the evaporation flux is greater (Matheny et al., 2014), and canopy roughness is more variable (Maurer et al., 2013) at the disturbed site than at the undisturbed sites. On seasonal timescales, mass balance dictates that the isotopic composition of transpired vapor must equal that of source water. On this relatively long timescale, we expect that the isotopic composition of transpired vapor was enriched in heavy isotopes relative to background vapor and that the greater transpiration flux at the undisturbed site pushed $\delta^{18}O$ within the canopy to higher values than at the disturbed site. Due to the fractionation associated with the evaporation of soil water that preferentially partitions lighter isotopologues into the vapor phase, more evaporation at the disturbed site depressed vapor $\delta^{18}O$ relative to the undisturbed site. Maurer et al. (2013) demonstrated that the structural rearrangement at the disturbed site altered the surface roughness parameters and increased surface drag, turbulent eddies, and vertical mixing. Although analysis of surface roughness did not continue past 2011, the lower observed $\delta^{18}O$ at the disturbed site suggests that between-site differences in vertical mixing persist at UMBS.

Species-specific hydrologic strategies may also have contributed to observed isotopic differences. Aspen transpire a majority of the water at the undisturbed site; absent this species at the disturbed site, oak and pine account for a much larger proportion of sap flux (Matheny et al., 2014). At UMBS, oak have a relatively deep rooting depth and access a deeper soil water pool that is more depleted in heavy isotopes than near-surface soil water (Matheny et al., 2016). Therefore, more transpiration from oak at the disturbed site may have contributed more isotopically negative vapor into the disturbed canopy than the undisturbed canopy. Differences in stomatal regulation may also control vapor isotopes because oak at UMBS are anisohydric while maple and aspen are isohydric (Matheny et al., 2016; Thomsen et al., 2013). While these species-specific hydrologic strategies may affect vapor isotopes, the trees at the two sites generally share much of the same physiology. Therefore, we focus on structural differences between the disturbed and undisturbed sites because the differences between the sites are greater.

4.2 Synoptic Variability

Isotope, sap flux, and eddy covariance data from the DOY 166-171 storm reveal synoptic scale differences in water cycling between the disturbed and undisturbed sites. Following the rainfall event, precipitation moved quickly through the porous sandy UMBS soil, was rapidly taken up by trees, and transpired to the atmosphere (He et al., 2013; Matheny et al., 2014; Nave et al., 2011). At the undisturbed site where transpiration dominates the ET flux (Figure 5b and

Matheny et al., 2014), T/ET, vapor $\delta^{18}O$, and $\delta^{18}O_{ET}$ increased after the storm. Due to increased light penetration and a more open canopy structure, evaporation played a larger role in the ET flux at the disturbed site. Accordingly, T/ET remained nearly unchanged immediately after the storm. At both sites soil evaporation contributed more to the ET flux a few days after the storm and likely drove T/ET, $\delta^{18}O$, and $\delta^{18}O_{ET}$ to lower values. $\delta^{18}O_{ET}$ was most similar at the two sites during (DOY 167) and immediately after (DOY 168) the storm when evaporation of intercepted precipitation, which was likely the same at the two sites, contributed to $\delta^{18}O_{ET}$ (Figure 5a). Following DOY 168 and likely the complete evaporation of intercepted water, differences in vegetation, canopy structure, and the relative magnitudes of evaporation and transpiration fluxes caused $\delta^{18}O_{ET}$ to diverge at the two sites.

Measurements of additional water pools would greatly improve an isotopic understanding of synoptic scale water cycling and are suggested for future studies. We assume that rainwater had a lower d and higher $\delta^{18}O$ than background vapor (Gat, 1996), but without an exact value of the isotopic composition of precipitation it is difficult to diagnose the shift in vapor $\delta^{18}O$ due to transpiration after a rain storm. Similarly, without knowledge of the isotopic composition of soil water, it is difficult to estimate the decrease in vapor isotopes from evaporation. Additionally, isotopic measurements of xylem water would clarify questions of rooting depth and the timescales over which trees access recent precipitation. Matheny et al. (2014 and 2016) have previously reported on the rapid ET response to rain at UMBS. Following a storm, isotopic measurements of precipitation, soil, and xylem water would enable a similar assessment of forest water cycling. Future synoptic-scale vapor isotope studies, especially those without sap flux or eddy covariance data, should consider these additional measurements imperative to fully understand vapor isotope data and forest water cycling.

4.3 Vertical Variability

Vertical isotope gradients within the canopies demonstrate the effects of entrainment and local ET at the disturbed and undisturbed sites (Figure 4). Local above-canopy temperature, relative humidity, and wind speed were similar at the two sites (Figures 3 and Figure 7), therefore we attribute differences in vertical gradients to forest structure. To this end, we compared isotope gradients at four time slices through the day (Figure 4): in the middle of the night (a and e) and mid-afternoon (c and g) when local meteorological and atmospheric conditions were relatively stable and in the early morning (b and f) and late afternoon (d and h) when conditions changed rapidly. When transpiration was low at night, atmospheric mixing shifted vapor d ($\delta^{18}O$) to higher (lower) values. In all three seasons, vertical isotope gradients were larger at the undisturbed site than the disturbed site and more pronounced at night when water fluxes were relatively low. With higher water fluxes and more turbulence through the day, entrained and transpired vapor was mixed through the canopies so that by sunset vertical isotopic gradients dissolved away (Figures 4d and 4h). This pattern was most pronounced during the summer sampling period and more distinguishable within the thick, spatially homogenous,

undisturbed canopy that is prone to stratification than within the open, disturbed canopy that has many gaps that promote mixing.

Differences in forest structure at the two sites also contributed to gradients of diurnal temperature, relative humidity, and VPD between the surface (2 m) and above the canopies (Figure 7). In general, these gradients were greater at the undisturbed site than at the disturbed site. At the undisturbed site, nighttime conditions near the surface were generally moister than at 34 m due to the thick canopy that slowed the advection of moisture from within the canopy to the free atmosphere above. In contrast, during the day at the disturbed site, the surface was slightly warmer and drier than conditions above the canopy. There, open gaps among the trees allowed more solar radiation to reach the forest floor and promoted vertical mixing (Hardiman et al., 2013).

4.4 Diurnal Isotope Variations

Diurnal water vapor isotope cycles have been widely reported and generally appear to be independent of continentality or vegetation type. Diurnal cycles of $\delta^{18}O$ and d at UMBS are similar to those observed in coastal New Haven (Lee, Kim, & Smith, 2007; Lee, Smith, & Williams, 2006), above a wheat field (Zhang, Sun, Wang, Yu, & Wen, 2011) and arid oasis cropland (Huang & Wen, 2014) in North China, in a coniferous forest in the Pacific Northwest (Lai & Ehleringer, 2011), above a Mediterranean coastal wetland (Delattre et al., 2015), in an evergreen forest in Northern California (Simonin et al., 2014), and in an isotope enabled large-eddy simulation of the atmospheric boundary layer (Lee, Huang, & Patton, 2012). Welp et al. (2012) reported on water vapor d from six sites in the United States and China, including a broadleaf deciduous forest site in Borden, Ontario near UMBS. While local water fluxes affect the magnitude of diurnal isotope cycles, characteristic patterns of diurnal $\delta^{18}O$ and d variation emerged in all of these locations. Taken together, these cycles reflect competing influences of boundary layer entrainment and local ET on near surface water vapor.

Generally, entrainment and evaporation mix vapor with high d and low $\delta^{18}O$ into a forest canopy. q helps differentiate these two processes as evaporation moistens canopy air and entrainment dries canopy air. On short (sub-hourly) timescales, the isotopic composition of transpired vapor depends on leaf and xylem water storage and local meteorological conditions. On diurnal timescales, relative humidity changes cause vapor d to increase in the morning and decrease in the evening (Simonin et al., 2014). As morning relative humidity decreases and evaporation increases, the degree of kinetic fractionation increases and acts to increase vapor d. This kinetic effect is driven by the diffusivity difference between isotopologues during evaporation (Cappa, 2003; Merlivat, 1978). Environmental conditions are the opposite in the evening and, following the same logic that explains equilibrium and kinetic fractionation factors in the morning, tend to decrease vapor d late in the day as relative humidity increases. As a result of daytime transpiration, leaf water undergoes an isotopic enrichment and is expected to have a low d by the late afternoon. During the late afternoon and evening when relative humidity is high

13

and transpiration likely occurs closer to equilibrium, stored leaf water with low d may also decrease vapor d.

A few features of the diurnal $\delta^{18}O$ and d cycles are consistent between sites, seasons, and heights and reflect the dominant hydrologic processes in the UMBS canopies. In the early morning, transpiration drove a small increase of $\delta^{18}O$ and decrease of d (Figure 7). These isotopic shifts began just after sunrise and coincided with a VPD increase and the initiation of diurnal sap flux. In the mid-morning d increased rapidly as sap flux increased, temperature increased, and relative humidity decreased. As temperature and relative humidity changed in the late afternoon and evening, d decreased as expected. At night, when sap flux and VPD were at minima, entrainment was low and d was generally consistent, the isotopic composition of canopy vapor was predominantly governed by equilibrium fractionation. We did not observe characteristic isotope patterns of dew formation at either site, perhaps due to the relatively thick canopy and high LAI (3 $m^2\,m^{-2}$) of the UMBS forest. Unlike some open-canopy forests (e.g. a ponderosa pine forest in central Colorado (Berkelhammer et al., 2013)), at UMBS dew formation did not impart a distinct signature on the isotopic composition of near surface water vapor.

At UMBS, transpiration dominates ET at the undisturbed site; evaporation accounts for a larger fraction of ET at the disturbed site (Matheny et al., 2014). In addition, due to differences in canopy structure, we expect that more entrained vapor was mixed into the disturbed canopy than into the undisturbed canopy (Maurer et al., 2013). At the undisturbed site, the early increase of summer q and d suggest that transpiration supplied most of the morning vapor within that canopy. The morning q increase was absent at the disturbed site because there was less transpiration at that site and more entrainment of dry air from above the canopy. By mid-day, higher wind speeds and warmer surface temperatures increased mechanical turbulence and buoyant convection and entrained vapor was mixed into both canopies. Entrainment tended to depress $\delta^{18}O$ of vapor within the disturbed canopy. It is likely that evaporation also decreased $\delta^{18}O$ at the disturbed site, but it is difficult to disentangle evaporation and entrainment because the variations of q were so small.

We further examined the controls on diurnal isotopic compositions with a $\delta^{18}O$-δD plot of diurnal summer water vapor measurements (Figure 8). In this dual isotope space, diurnal vapor isotopic measurements produce a hysteretic loop that readily demonstrates when equilibrium and kinetic fractionation dominated in the UMBS canopies and highlights hydrologic differences at the disturbed and undisturbed sites. In the early morning, transpiration briefly drove $\delta^{18}O$ and δD higher and likely shifted vapor isotopes toward the isotopic composition of xylem water. This feature of the $\delta^{18}O$-δD hysteric loop is more pronounced at the undisturbed site where the transpiration flux was greater and the thicker canopy initially retained transpired vapor and slowed the intrusion of entrained vapor. d increased through the morning at both sites, but the kinetic effect was stronger (compare the slope between ~9 am and just before noon) at the disturbed site, which is consistent with a greater contribution of evaporated vapor. At noon, $\delta^{18}O$ values were ~ -19‰ at the two sites. Through the afternoon, entrainment and ET pushed isotopic compositions to lower values, although this effect was greater at the disturbed

site (-2‰) than at the undisturbed site (-1‰) likely due to differences in canopy structure. In the late afternoon and evening, transpiration dragged isotopic compositions up to similar nighttime values (~ -19‰). The evening shift from decreasing isotope values to increasing isotope values occurred approximately three hours later at the undisturbed site than at the disturbed site (compare the direction of the hysteric loop after 6 pm). The thick, closed undisturbed canopy was slow to change and retained daytime characteristics well into the evening. Alternatively, the open, disturbed canopy responded rapidly to changing atmospheric and meteorological conditions.

4.5 Summertime Surface-Atmosphere Vapor Mixing

Finally, we focus on summertime meteorological and isotopic differences within and above the disturbed and undisturbed canopies and examine the implications of intermediate disturbance on forest hydrology. We concentrate on the summer period because differences in canopy structure at the two sites were most pronounced during this time. At the disturbed site, summer temperature, VPD, and vapor isotopic compositions were nearly identical within and above the canopy (Figure 2 i-m). Alternatively, when vertical temperature and relative humidity gradients emerged at the undisturbed site, for example during DOY 161-163, 166-173, and 175-179, isotopic gradients emerged as well (Figure 2a-f). In particular, above-canopy d deviated from within-canopy d during these times (Figure 2c). The timing of summer vertical meteorological and isotope gradients suggests that, at times, air above the undisturbed canopy was incompletely mixed with air within the canopy. During the summer, air at the disturbed site generally remained well mixed from the surface to at least 32 m.

Diurnal summer isotopes and meteorology at the undisturbed site also point to a decoupling between water vapor within the canopy and vapor above the canopy. Above the undisturbed canopy, d and q exhibited similar diurnal patterns and were strongly correlated (Pearson's r > 0.8, Figures 7r and 7s). The coherence between diurnal d and q was unique to the 34 m observations at the undisturbed site, and points to a measurable influence of canopy structure on forest water cycling. The correlation between d and q was low (r < 0.5) at all other sampling locations. In addition, the disturbance muted diurnal vertical meteorological gradients (Figure 7), and suggests that forest structure affects mixing within the canopy. Broadly, this suggests that the assumption of well-coupled canopy-atmosphere interactions (e.g. Ewers & Oren, 2000) may be violated in the case of thick, homogeneous forest canopies.

4.6 Implications of Intermediate Disturbance on Forest Hydrology

Since its initiation in 2008, the FASET disturbance has proven to be a fruitful experiment to examine and better understand forest biogeochemical responses to intermediate disturbances such as forest thinning management or rapid ecological succession. Following the treatment, carbon, nitrogen, and water cycles changed rapidly in the disturbed plot. Carbon (Gough et al., 2013) and nitrogen (Nave et al., 2011) cycles returned to pre-treatment levels within a few years; changes to boundary layer turbulence (Maurer et al., 2013), forest structure (Hardiman et al.,

2013) and the water cycle (He et al., 2013; Matheny et al., 2014) have persisted. Here we use water vapor isotopes to demonstrate that intermediate disturbances that open canopy gaps can alter vapor mixing within and above a forest canopy. Our results also show that forest canopy structure modulates the timescale over which moisture is returned to the atmosphere, as closed canopies can act like a diffusive boundary layer and return energy and moisture to the atmosphere more slowly than open canopies. Greater vapor mixing between the surface layer and the above-canopy layer may increase moisture transport as surface layer moisture is mixed into the drier above-canopy air and advected away, and therefore may influence the timing and amount of downstream moisture. At the local scale, increased surface-atmosphere water vapor mixing may reduce forest moisture retention and further influence forest composition (Fotis et al., 2018). Many of these inferences can be made from eddy covariance, sap flux, or vapor isotope measurements. However, only isotopes offer insights into the particular processes, both during the day and at night, that generate water fluxes.

Importantly, forest intermediate disturbances do not proceed in isolation. Instead, over the next few decades, many forests will experience higher atmospheric CO_2 and warmer temperatures. It is therefore prudent to consider disturbance alongside the broad suite of pressures that may affect forests. Independent of atmospheric CO_2, changes in vertical mixing modulated by canopy structure can increase VPD and impact stomatal regulation, transpiration, and photosynthesis (Novick et al., 2016). Under higher atmospheric CO_2, decreased stomatal conductance may increase intrinsic water-use efficiency (Frank et al., 2015). Under higher CO_2 conditions, many climate models suggest that transpiration will decrease or remain stable (Lemordant, Gentine, Swann, Cook, & Scheff, 2018; Skinner, Poulsen, Chadwick, Diffenbaugh, & Fiorella, 2017). Although many changes to forest water cycles, including stomatal behavior, forest moisture gradients, and soil wetness, are yet unknown, higher water-use efficiency and increased canopy openness may reinforce each other to further dry forest environments. If the transpiration rate remains stable as canopies transition from closed to open, more canopy moisture may be lost to the atmosphere, which may increase the flux of water from forests to downstream regions.

5 Conclusions

We compared meteorology, sap flux, and vertical profiles of water vapor stable isotopes in two closely located forest sites in northern Michigan to assess the effects of intermediate disturbance and canopy structure on local hydrologic cycling. Records from both the disturbed and undisturbed sites reflect seasonality and are imprinted with storm events. On diurnal timescales, we found that differences in water vapor isotope cycles reflect differences in canopy structure, the relative influence of entrainment and ET, and the hydrologic mixing both within the canopy and between the surface layer and the atmosphere. These differences were most pronounced during the summer when the canopies were fully developed and transpiration was high. Vertical water vapor isotope measurements revealed stratified canopy vapor at night at the undisturbed site and relatively well mixed canopy air at the disturbed site. Generally,

16

meteorological, sap flux, and isotopic measurements complement each other: eddy covariance gives the net water flux and isotopes reveal the hydrologic processes that generate that flux. This work helps expand our understanding of water vapor isotopes in forests and improves predictions of water fluxes between the land and atmosphere and associated changes to regional climate and water cycles.

Acknowledgments

Figure 1. δ^{18}O (‰) and δD (‰) of water vapor measured during all three sampling periods at a) the undisturbed site (green) and b) the disturbed site (blue). Color intensity increases for each seasonal period from spring (pale) to fall (dark). For reference, the GMWL is plotted as a black line.

Figure 2. Time series of moving 24-hour average of summer isotopic compositions, meteorological data, and sap flux at the undisturbed (left) and disturbed (right) sites. a,i) vapor δ^{18}O (‰); b,j) d (‰); c,k) specific humidity (q, g/kg); d,l) temperature (°C); e,m) vapor pressure deficit (VPD, kPa); f,n) wind speed (m/s); g,o) sap flux (W/m^2); h,p) daily precipitation amount (mm). Isotopes and specific humidity are shown for all 6 heights from low (red) to high (blue). Meteorology is shown at 2 m (red) and above-canopy (blue).

Figure 3. Differences (Δ, undisturbed – disturbed) between the undisturbed and disturbed sites in the spring (a-h), summer (i-p), and fall (q-x). a,i,q) vapor δ^{18}O (‰); b,j,r) d (‰); c,k,s) specific

humidity (q, g/kg); d,l,t) temperature (°C); e,m,u) vapor pressure deficit (VPD, kPa); f,n,v) wind speed (m/s); g,o,w) sap flux (W/m^2). Panels h, p, and x show total daily precipitation amount (mm). Differences of isotopes and specific humidity are shown for all 6 heights from low (red) to high (blue). Where measured, meteorological differences are shown at 2 m (red) and above-canopy (blue).

Figure 4. Mean profiles of water vapor δ^{18}O (‰) from the undisturbed (green) and disturbed (blue) sites during the spring, summer, and fall. Shown here are profiles from four time slices: nighttime (00:00 to 03:00, a and e), sunrise (06:00 to 09:00, b and f), midafternoon (14:00 to 17:00, c and g), and sunset (18:00 to 21:00, d and h). Grey shading indicates heights above the canopy. Error bars show standard error.

Figure 5. a) δ^{18}O$_{ET}$ and b) T/ET at the disturbed (blue) and undisturbed (green) sites during the summer storm (DOY 166-171). Rain fell during the day on DOY 167.

Figure 6. Time series of moving 24-hour average of summer storm (DOY 166-171). Rain fell on DOY 167. a,e) vapor δ^{18}O (‰); b,f) specific humidity (q, g/kg); c,g) vapor pressure deficit (VPD, kPa); d,h) sap flux (W/m^2) at the undisturbed (left) and disturbed (right) sites. Isotopes and specific humidity are shown for all 6 heights from low (red) to high (blue). Meteorology is shown at 2 m (red) and above-canopy (blue).

Table 1. Isotopic, meteorologic, and sap flux differences between the undisturbed and disturbed sites. Statistical significance ($p < 0.05$) is indicated by bolded values.

Figure 7. Diurnal isotopic, meteorologic, and sap flux cycles at all sampling heights in the spring (a-p), summer (q-af), and fall (ag-av). Diurnal cycles were calculated by removing the background isotopic composition at 15 m. In each season, diurnal cycles at the undisturbed site are shown on the left (a-h, q-x, and ag-an) and diurnal cycles from the disturbed site are to the right (i-p, y-af, and ao-av). δ^{18}O (‰), (a,i,q,y,ag,ao); d (‰), (b,j,r,z,ah,ap); q (g/kg), (c,k,s,aa,ai,aq); temperature (°C), (d,l,t,ab,aj,ar); relative humidity (%), (e,m,u,ac,ak,as); vapor pressure deficit (VPD, kPa), (f,n,v,ad,al,at); wind speed (m/s), (g,o,w,ae,am,au); and sap flux (W/m^2), (h,p,x,af,an,av) are shown for both sites and all three seasons. Heights of isotope measurements vary along a spectrum from low (red) to high (blue) height. Meteorological variables were measured near the surface (red) and above the canopy (blue).

Figure 8. 15 m interpolated diurnal summer δ^{18}O and δD from the undisturbed (top) and disturbed (bottom) sites. Each diurnal δ^{18}O and δD value was interpolated to a five-minute time step to demonstrate the hysteretic loop of water vapor δ^{18}O and δD throughout the day. Color indicates time and varies from midnight (navy) to morning, afternoon, and night (yellow, green, and blue, respectively). White, grey, and black circles indicate 6 am, 12 pm, and 6 pm,

respectively. The red circle indicates midnight. Arrows indicate hydrologic processes that drive the isotopic composition of water vapor within the canopies and point in the direction that each process pushes isotope values. The global meteoric water line (GMWL) is included for reference.

References

Aemisegger, F., Pfahl, S., Sodemann, H., Lehner, I., Seneviratne, S. I., & Wernli, H. (2014). Deuterium excess as a proxy for continental moisture recycling and plant transpiration. *Atmospheric Chemistry and Physics*, *14*(8), 4029–4054. https://doi.org/10.5194/acp-14-4029-2014

Aemisegger, F., Sturm, P., Graf, P., Sodemann, H., Pfahl, S., Knohl, A., & Wernli, H. (2012). Measuring variations of $\delta^{18}O$ and $\delta^{2}H$ in atmospheric water vapour using two commercial laser-based spectrometers: an instrument characterisation study. *Atmospheric Measurement Techniques*, *5*, 1491–1511. https://doi.org/10.5194/amt-5-1491-2012

Anderegg, W. R. L., Konings, A. G., Trugman, A. T., Yu, K., Bowling, D. R., Karp, D., et al. (2018). Hydraulic diversity of forests regulates ecosystem resilience during drought. *Nature*, *561*(7724), 537–541. https://doi.org/10.1038/s41586-018-0539-7

Asase, A., Asiatokor, B. K., & Ofori-Frimpong, K. (2014). Effects of selective logging on tree diversity and some soil characteristics in a tropical forest in southwest Ghana. *Journal of Forestry Research*, *25*(1), 171–176. https://doi.org/10.1007/s11676-014-0443-4

Asner, G. P., Keller, M., Pereira, R., Zweede, J. C., & Silva, J. N. M. (2004). Canopy damage and recovery following selective logging in an Amazon forest: Integrating field and satellite studies. *Ecological Applications*, *14*(4), 280–298. https://doi.org/https://doi.org/10.1890/01-6019

Atkins, J. W., Fahey, R. T., Hardiman, B. H., & Gough, C. M. (2018). Forest Canopy Structural Complexity and Light Absorption Relationships at the Subcontinental Scale. *Journal of Geophysical Research: Biogeosciences*, *123*(4), 1387–1405. https://doi.org/10.1002/2017JG004256

Bailey, A., Noone, D., Berkelhammer, M., Steen-Larsen, H. C., & Sato, P. (2015). The stability and calibration of water vapor isotope ratio measurements during long-term deployments. *Atmospheric Measurement Techniques*, *8*(10), 4521–4538. https://doi.org/10.5194/amt-8-4521-2015

Baldocchi, D. D., & Meyers, T. (1998). On using eco-physiological, micrometeorological and biogeochemical theory to evaluate carbon dioxide, water vapor and trace gas fluxes over

vegetation: a perspective. *Agricultural and Forest Meteorology*, *90*, 1–25. https://doi.org/10.1016/S0168-1923(97)00072-5

Baldocchi, D. D., Wilson, K. B., & Gu, L. (2002). How the environment, canopy structure and canopy physiological functioning influence carbon, water and energy fluxes of a temperate broad-leaved deciduous forest - An assessment with the biophysical model CANOAK. *Tree Physiology*, *22*(15–16), 1065–1077. https://doi.org/10.1093/treephys/22.15-16.1065

Barnes, C. J., & Allison, G. . (1984). The distribution of deuterium and 18O in dry soils: 3. Theory for non-isothermal water movement. *Journal of Hydrology*, *74*, 119–135. https://doi.org/10.1016/0022-1694(84)90144-6

Berkelhammer, M., Hu, J., Bailey, A., Noone, D. C., Still, C. J., Barnard, H., et al. (2013). The nocturnal water cycle in an open-canopy forest. *Journal of Geophysical Research Atmospheres*, *118*(17), 10225–10242. https://doi.org/10.1002/jgrd.50701

Cappa, C. D. (2003). Isotopic fractionation of water during evaporation. *Journal of Geophysical Research*, *108*(D16), 4525. https://doi.org/10.1029/2003JD003597

Cernusak, L. A., Pate, J. S., & Farquhar, G. D. (2002). Diurnal variation in the stable isotope composition of water and dry matter in fruiting Lupinus angustifolius under field conditions. *Plant, Cell and Environment*, *26*, 893–907. https://doi.org/10.1046/j.1365-3040.2002.00875.x

Chen, J., Saunders, S. C., Crow, T. R., Naiman, R. J., Kimberley, D., Mroz, G. D., et al. (1999). Microclimate in Forest Ecosystem and Landscape Ecology. *BioScience*, *49*(4), 288–297. https://doi.org/10.2307/1313612

Craig, H. (1961). Isotopic Variations in Meteoric Waters. *Science*, *133*(3465), 1702–1703. https://doi.org/10.1126/science.133.3465.1702

Dansgaard, W. (1964). Stable isotopes in precipitation. *Tellus*, *16*(4), 436–468. https://doi.org/10.3402/tellusa.v16i4.8993

Debortoli, N. S., Dubreuil, V., Hirota, M., Filho, S. R., Lindoso, D. P., & Nabucet, J. (2017). Detecting deforestation impacts in Southern Amazonia rainfall using rain gauges. *International Journal of Climatology*, *37*(6), 2889–2900. https://doi.org/10.1002/joc.4886

Delattre, H., Vallet-Coulomb, C., & Sonzogni, C. (2015). Deuterium excess in the atmospheric water vapour of a Mediterranean coastal wetland: Regional vs. local signatures. *Atmospheric Chemistry and Physics*, *15*(17), 10167–10181. https://doi.org/10.5194/acp-15-10167-2015

Ehleringer, J. R., & Dawson, T. E. (1992). Water uptake by plants: perspectives from stable isotope composition. *Plant, Cell and Environment*, *15*, 1073–1082. https://doi.org/10.1111/j.1365-3040.1992.tb01657.x

Ellison, D., Morris, C. E., Locatelli, B., Sheil, D., Cohen, J., Murdiyarso, D., et al. (2017). Trees, forests and water: Cool insights for a hot world. *Global Environmental Change*, *43*, 51–61. https://doi.org/10.1016/j.gloenvcha.2017.01.002

Ewers, B. E., & Oren, R. A. M. (2000). Analyses of assumptions and errors in the calculation of stomatal conductance from sap flux measurements. *Tree Physiology*, *20*, 579–589.

Fiorella, R. P., Bares, R., Lin, J. C., Ehleringer, J. R., & Bowen, G. J. (2018). Detection and variability of combustion-derived vapor in an urban basin. *Atmospheric Chemistry and Physics*, *18*(12), 8529–8547. https://doi.org/10.5194/acp-18-8529-2018

Fiorella, R. P., Poulsen, C. J., & Matheny, A. M. (2018). Seasonal Patterns of Water Cycling in a Deep, Continental Mountain Valley Inferred From Stable Water Vapor Isotopes. *Journal of Geophysical Research: Atmospheres*, *123*(14), 7271–7291. https://doi.org/10.1029/2017JD028093

Fotis, A. T., Morin, T. H., Fahey, R. T., Hardiman, B. S., Bohrer, G., & Curtis, P. S. (2018). Forest structure in space and time: Biotic and abiotic determinants of canopy complexity and their effects on net primary productivity. *Agricultural and Forest Meteorology*, *250–251*(June 2017), 181–191. https://doi.org/10.1016/j.agrformet.2017.12.251

Frank, D. C., Poulter, B., Saurer, M., Esper, J., Huntingford, C., Helle, G., & Treydte, K. (2015). Water-use efficiency and transpiration across European forests during the Anthropocene. *Nature Climate Change*, *5*, 579–584. https://doi.org/10.1038/NCLIMATE2614

Galewsky, J., & Samuels-Crow, K. (2015). Summertime moisture transport to the southern South American Altiplano: Constraints from in situ measurements of water vapor isotopic composition. *Journal of Climate*, *28*(7), 2635–2649. https://doi.org/10.1175/JCLI-D-14-00511.1

Ganteaume, A., Camia, A., Jappiot, M., San-Miguel-Ayanz, J., Long-Fournel, M., & Lampin, C. (2013). A review of the main driving factors of forest fire ignition over Europe. *Environmental Management*, *51*(3), 651–662. https://doi.org/10.1007/s00267-012-9961-z

Gat, J. (1996). Oxygen and hydrogen isotopes in the hydrologic cycle. *Annual Review of Earth and Planetary Sciences*, *24*, 225–262. https://doi.org/10.1146/annurev.earth.24.1.225

Gat, J. R., Bowser, C. J., & Kendall, C. (1994). The contribution of evaporation from the Great

21

Lakes to the continental atmosphere: estimate based on stable isotope data. *Geophysical Research Letters*, *21*(7), 557–560. https://doi.org/10.1029/94GL00069

Good, S. P., Soderberg, K., Guan, K., King, E. G., Scanlon, T. M., & Caylor, K. K. (2014). δ^2H isotopic flux partitioning of evapotranspiration over a grass field following a water pulse and subsequent dry down. *Water Resources Research*, *50*, 1410–1432. https://doi.org/10.1002/2013WR014333

Gough, C. M., Hardiman, B. S., Nave, L. E., Bohrer, G., Maurer, K. D., Vogel, C. S., et al. (2013). Sustained carbon uptake and storage following moderate disturbance in a Great Lakes forest. *Ecological Applications*, *23*(5), 1202–1215. https://doi.org/10.1890/12-1554.1

Granier, A. (1987). Evaluation of transpiration in a Douglas-fir stand by means of sap flow measurements. *Tree Physiology*, *3*(4), 309–320. https://doi.org/10.1093/treephys/3.4.309

Hardiman, B. S., Bohrer, G., Gough, C. M., & Curtis, P. S. (2013). Canopy structural changes following widespread mortality of canopy dominant trees. *Forests*, *4*(3), 537–552. https://doi.org/10.3390/f4030537

Hardiman, B. S., LaRue, E. A., Atkins, J. W., Fahey, R. T., Wagner, F. W., & Gough, C. M. (2018). Spatial variation in canopy structure across forest landscapes. *Forests*, *9*(8). https://doi.org/10.3390/f9080474

Harwood, K. G., Gillon, J. S., Griffiths, H., & Broadmeadow, M. S. J. (1998). Diurnal variation of $\Delta^{13}CO_2$, $\Delta^{18}O^{16}O$ and evaporative site enrichment of $\delta H_2^{18}O$ in Piper aduncum under field conditions in Trinidad. *Plant, Cell and Environment*, *21*(3), 269–283. https://doi.org/10.1046/j.1365-3040.1998.00276.x

He, H. S., & Mladenoff, D. J. (1999). Spatially Explicit and Stochastic Forest Landscape Model of Fire Disturbance and Succession. *Ecology*, *80*(1), 81–99. https://doi.org/10.2307/176981

He, H., & Smith, R. B. (1999). Stable isotope composition of water vapor in the atmospheric boundary layer above the forests of New England. *Journal of Geophysical Research Atmospheres*, *104*(D9), 11657–11673. https://doi.org/10.1029/1999JD900080

He, L., Ivanov, V. Y., Bohrer, G., Thomsen, J. E., Vogel, C. S., & Moghaddam, M. (2013). Temporal dynamics of soil moisture in a northern temperate mixed successional forest after a prescribed intermediate disturbance. *Agricultural and Forest Meteorology*, *180*, 22–33. https://doi.org/10.1016/j.agrformet.2013.04.014

Herms, D. A., & McCullough, D. G. (2014). Emerald Ash Borer Invasion of North America: History, Biology, Ecology, Impacts, and Management. *Annual Review of Entomology*,

59(1), 13–30. https://doi.org/10.1146/annurev-ento-011613-162051

Hesslerová, P., Pokorný, J., Brom, J., & Rejšková-Procházková, A. (2013). Daily dynamics of radiation surface temperature of different land cover types in a temperate cultural landscape: Consequences for the local climate. *Ecological Engineering*, *54*, 145–154. https://doi.org/10.1016/j.ecoleng.2013.01.036

Horita, J., & Wesolowski, D. J. (1994). Liquid-vapor fractionation of oxygen and hydrogen isotopes of water from the freezing to the critical temperature. *Geochimica et Cosmochimica Acta*, *58*(16), 3425–3437. Retrieved from papers2://publication/uuid/F9BCD32F-8569-4ACF-81AF-08518BF40A32

Huang, L., & Wen, X. (2014). Temporal variations of atmospheric water vapor δD and $\delta^{18}O$ above an arid artifical oasis cropland in the Heihe River Basin. *Journal of Geophysical Research: Atmospheres*, *119*, 11,456-11,476. https://doi.org/10.1002/2014JD021891

Jasechko, S., Sharp, Z. D., Gibson, J. J., Birks, S. J., Yi, Y., & Fawcett, P. J. (2013). Terrestrial water fluxes dominated by transpiration. *Nature*, *496*(7445), 347–350. https://doi.org/10.1038/nature11983

Keeling, D. (1958). The concentration and isotopic abundances of atmospheric carbon dioxide in rural areas. *Geochimica et Cosmochimica Acta*, *13*, 322–334.

Lai, C. T., & Ehleringer, J. R. (2011). Deuterium excess reveals diurnal sources of water vapor in forest air. *Oecologia*, *165*(1), 213–223. https://doi.org/10.1007/s00442-010-1721-2

Lee, X., Huang, J., & Patton, E. G. (2012). A Large-Eddy Simulation Study of Water Vapour Boundary Layer, 229–248. https://doi.org/10.1007/s10546-011-9631-3

Lee, X., Kim, K., & Smith, R. (2007). Temporal variations of the $^{18}O/^{16}O$ signal of the whole-canopy transpiration in a temperate forest, *21*(August), 1–12. https://doi.org/10.1029/2006GB002871

Lee, X., Smith, R., & Williams, J. (2006). Water vapour $^{18}O/^{16}O$ isotope ratio in surface air in New England, USA. *Tellus B: Chemical and Physical Meteorology*, *58*(4), 293–304. https://doi.org/10.1111/j.1600-0889.2006.00191.x

Lemordant, L., Gentine, P., Swann, A. S., Cook, B. I., & Scheff, J. (2018). Critical impact of vegetation physiology on the continental hydrologic cycle in response to increasing CO_2. *Proceedings of the National Academy of Sciences*, *115*(16), 4093–4098. https://doi.org/10.1073/pnas.1720712115

Logan, J. A., Régnière, J., & Powell, J. A. (2003). Assessing the impacts of global warming on forest pest dynamics. *Frontiers in Ecology and the Environment*, *1*(3), 130–137. https://doi.org/110.1890/1540-9295(2003)001[0130:ATIOGW]2.0.CO;2

Luz, B., Barkan, E., Yam, R., & Shemesh, A. (2009). Fractionation of oxygen and hydrogen isotopes in evaporating water. *Geochimica et Cosmochimica Acta*, *73*(22), 6697–6703. https://doi.org/10.1016/j.gca.2009.08.008

Matheny, A. M., Bohrer, G., Vogel, C. S., Morin, T. H., He, L., Frasson, R. P. D. M., et al. (2014). Species-specific transpiration responses to intermediate disturbance in a northern hardwood forest. *Journal of Geophysical Research: Biogeosciences*, *119*, 2292–2311. https://doi.org/10.1002/2014JG002804

Matheny, A. M., Fiorella, R. P., Bohrer, G., Poulsen, C. J., Morin, T. H., Wunderlich, A., et al. (2016). Contrasting strategies of hydraulic control in two codominant temperate tree species. *Ecohydrology*, *10*(3), 1–16. https://doi.org/10.1002/eco.1815

Maurer, K. D., Hardiman, B. S., Vogel, C. S., & Bohrer, G. (2013). Canopy-structure effects on surface roughness parameters: Observations in a Great Lakes mixed-deciduous forest. *Agricultural and Forest Meteorology*, *177*, 24–34. https://doi.org/10.1016/j.agrformet.2013.04.002

McDowell, N., Pockman, W. T., Allen, C. D., Breshears, D. D., Cobb, N., Kolb, T., et al. (2008). Mechanisms of Plant Survival and Mortality during Drought : Why Do Some Plants Survive while Others Succumb to Drought? *New Phytologist*, *178*(4), 719–739. https://doi.org/10.1111/j.1469-8137.2008.02436.x

Merlivat, L. (1978). Molecular diffusivities of $H_2^{16}O$, $HD^{16}O$, and $H_2^{18}O$ in gases. *The Journal of Chemical Physics*, *69*(6), 2864–2871. https://doi.org/10.1063/1.436884

Mitchell, S. J. (2013). Wind as a natural disturbance agent in forests: A synthesis. *Forestry*, *86*(2), 147–157. https://doi.org/10.1093/forestry/cps058

Nave, L. E., Gough, C. M., Maurer, K. D., Bohrer, G., Hardiman, B. S., Le Moine, J., et al. (2011). Disturbance and the resilience of coupled carbon and nitrogen cycling in a north temperate forest. *Journal of Geophysical Research: Biogeosciences*, *116*(4), 1–14. https://doi.org/10.1029/2011JG001758

Noone, D., Risi, C., Bailey, A., Berkelhammer, M., Brown, D. P., Buenning, N., et al. (2013). Determining water sources in the boundary layer from tall tower profiles of water vapor and surface water isotope ratios after a snowstorm in Colorado. *Atmospheric Chemistry and Physics*, *13*(3), 1607–1623. https://doi.org/10.5194/acp-13-1607-2013

Novick, K. A., Ficklin, D. L., Stoy, P. C., Williams, C. A., Bohrer, G., Oishi, A. C., et al. (2016). The increasing importance of atmospheric demand for ecosystem water and carbon fluxes. *Nature Climate Change*, *6*(September), 1023–1027. https://doi.org/10.1038/NCLIMATE3114

Organization, F. and A. (2015). *Global Forest Resources Assessment 2015* (2nd ed.). Rome. Retrieved from http://www.fao.org/forestry/fra2005/en/

Pan, Y., Chen, J. M., Birdsey, R., McCullough, K., He, L., & Deng, F. (2011). Age structure and disturbance legacy of North American forests. *Biogeosciences*, *8*(3), 715–732. https://doi.org/10.5194/bg-8-715-2011

Parsons, D. J., & DeBenedetti, S. H. (1979). Impact of fire suppression on a mixed conifer forest. *Forest Ecology and Management*, *2*, 21–33.

Rasmusson, E. M. (1968). Atmospheric Water Vapor Transport and the Water Balance of North America. *Monthly Weather Review*, *96*(10), 720–734. https://doi.org/10.1175/1520-0493(1968)096<0720:AWVTAT>2.0.CO;2

Schlesinger, W. H., & Jasechko, S. (2014). Transpiration in the global water cycle. *Agricultural and Forest Meteorology*, *189–190*, 115–117. https://doi.org/10.1016/j.agrformet.2014.01.011

Schulte, L. A., Mladenoff, D. J., Crow, T. R., Merrick, L. C., & Cleland, D. T. (2007). Homogenization of northern U.S. Great Lakes forests due to land use. *Landscape Ecology*, *22*(7), 1089–1103. https://doi.org/10.1007/s10980-007-9095-5

Simonin, K. A., Link, P., Rempe, D., Miller, S., Oshun, J., Bode, C., et al. (2014). Vegetation induced changes in the stable isotope composition of near surface humidity. *Ecohydrology*, *7*(3), 936–949. https://doi.org/10.1002/eco.1420

Simonin, K. A., Roddy, A. B., Link, P., Apodaca, R., Tu, K. P., Hu, J., et al. (2013). Isotopic composition of transpiration and rates of change in leaf water isotopologue storage in response to environmental variables. *Plant, Cell and Environment*, *36*(12), 2190–2206. https://doi.org/10.1111/pce.12129

Skinner, C. B., Poulsen, C. J., Chadwick, R., Diffenbaugh, N. S., & Fiorella, R. P. (2017). The Role of Plant CO2 Physiological Forcing in Shaping Future Daily-Scale Precipitation. *Journal of Climate*, *30*(7), 2319–2340. https://doi.org/10.1175/JCLI-D-16-0603.1

Steen-Larsen, H. C., Sveinbjörnsdottir, A. E., Jonsson, T., Ritter, F., Bonne, J., Sodemann, H., et al. (2015). Moisture sources and synoptic to seasonal variability of North Atlantic water

vapor isotopic composition. *Journal Geophysical Research Atmospheres*, *120*, 5757–5774. https://doi.org/10.1002/2015JD023234

Stephens, S. L., Moghaddas, J. J., Edminster, C., Fiedler, C. E., Haase, S., Harrington, M. G., et al. (2009). Fire Treatment Effects on Vegetation Structure, Fuels, and Potential Fire Severity in Western U.S. Forests. *Ecological Applications*, *19*(2), 305–320. https://doi.org/10.1890/07-1755.1

Thomsen, J. E., Bohrer, G., Matheny, A. M., Ivanov, V. Y., He, L., Renninger, H. J., & Schäfer, K. V. R. (2013). Contrasting hydraulic strategies during dry soil conditions in Quercus rubra and Acer rubrum in a sandy site in Michigan. *Forests*, *4*(4), 1106–1120. https://doi.org/10.3390/f4041106

Trugman, A. T., Medvigy, D., Anderegg, W. R. L., & Pacala, S. W. (2018). Differential declines in Alaskan boreal forest vitality related to climate and competition. *Global Change Biology*, *24*(3), 1097–1107. https://doi.org/10.1111/gcb.13952

Welp, L. R., Lee, X., Griffis, T. J., Wen, X. F., Xiao, W., Li, S., et al. (2012). A meta-analysis of water vapor deuterium-excess in the midlatitude atmospheric surface layer. *Global Biogeochemical Cycles*, *26*(3), 1–12. https://doi.org/10.1029/2011GB004246

Welp, L. R., Lee, X., Kim, K., Griffis, T. J., Billmark, K. A., & Baker, J. M. (2008). δ^{18}O of water vapour, evapotranspiration and the sites of leaf water evaporation in a soybean canopy. *Plant, Cell and Environment*, *31*(9), 1214–1228. https://doi.org/10.1111/j.1365-3040.2008.01826.x
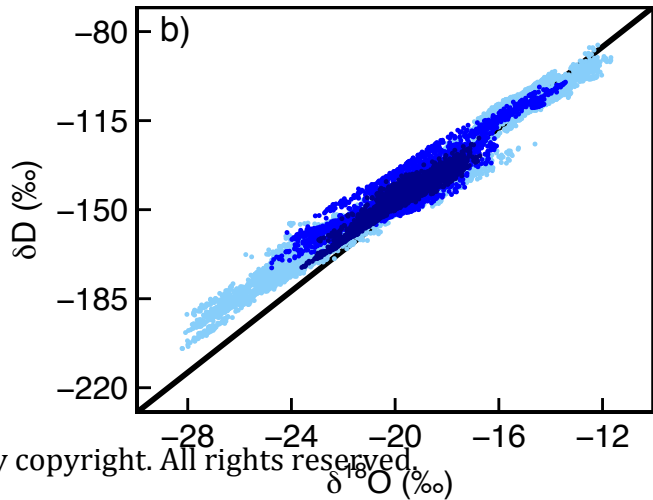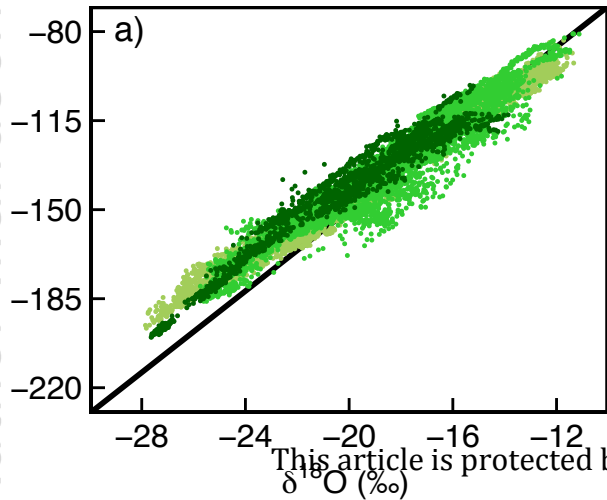
Williams, D. G., Cable, W., Hultine, K., Hoedjes, J. C. B., Yepez, E. A., Simonneaux, V., et al. (2004). Evapotranspiration components determined by stable isotope, sap flow and eddy covariance techniques. *Agricultural and Forest Meteorology*, *125*, 241–258. https://doi.org/10.1016/j.agrformet.2004.04.008

Xiao, W., Wei, Z., & Wen, X. (2018). Evapotranspiration partitioning at the ecosystem scale using the stable isotope method—A review. *Agricultural and Forest Meteorology*, *263*(November 2017), 346–361. https://doi.org/10.1016/j.agrformet.2018.09.005
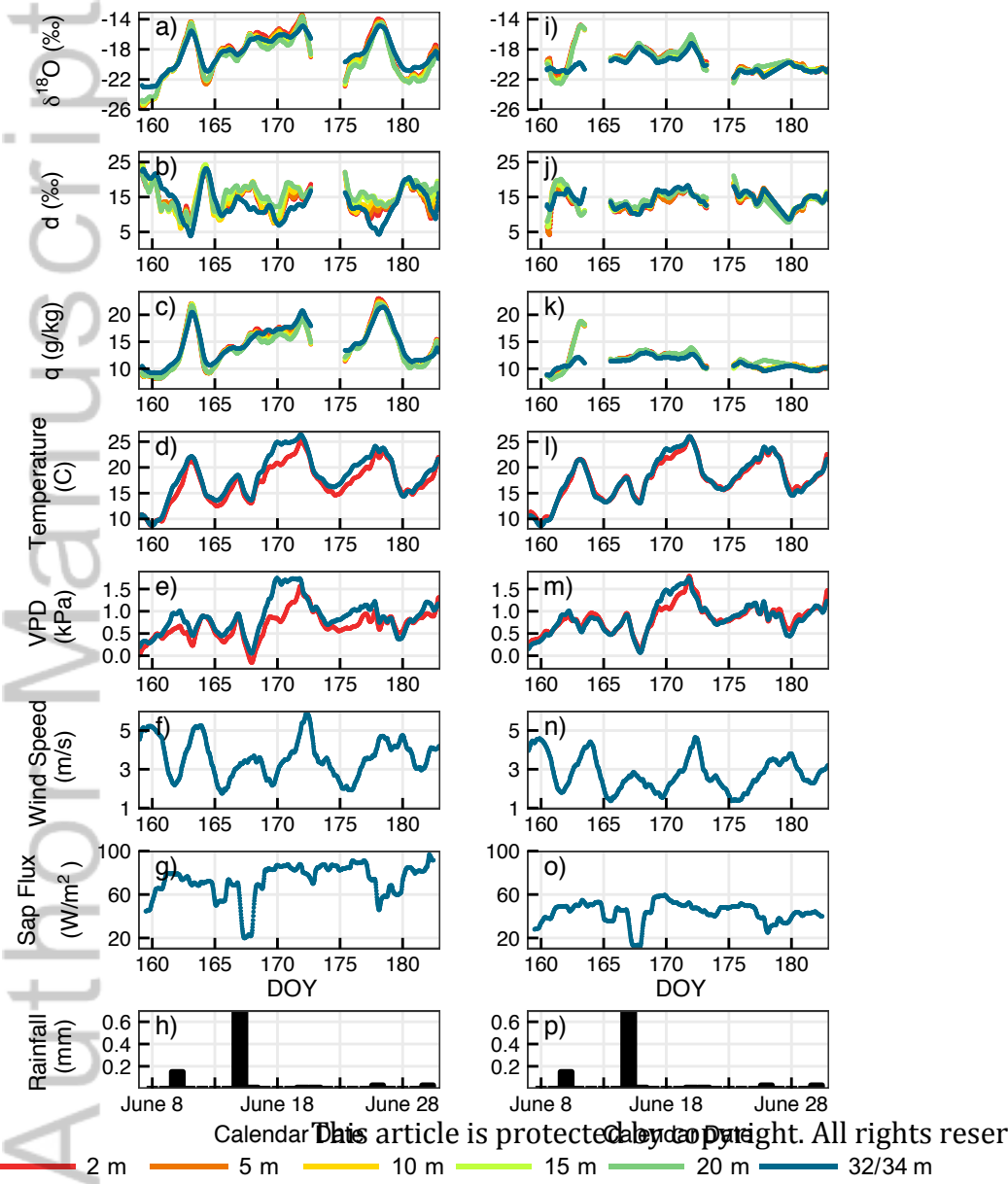
Yakir, D., & Sternberg, S. L. (2000). The use of stable isotopes to study ecosystem gas exchange, *123*(January), 297–311.
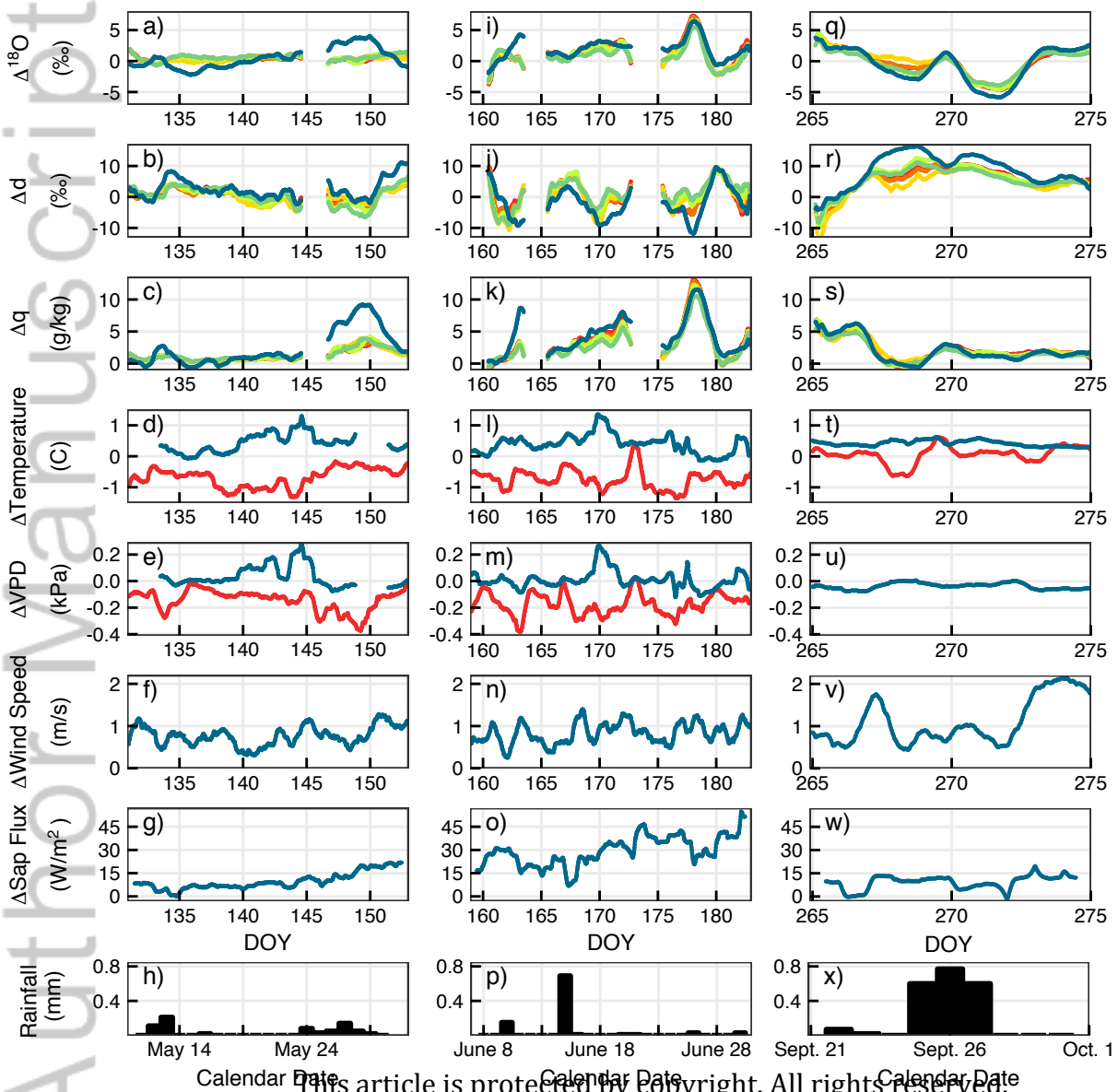
Zhang, S., Sun, X., Wang, J., Yu, G., & Wen, X. (2011). Short-term variations of vapor isotope ratios reveal the influence of atmospheric processes. *Journal of Geographical Sciences*, *21*(3), 401–416. https://doi.org/10.1007/s11442-011-0853-6
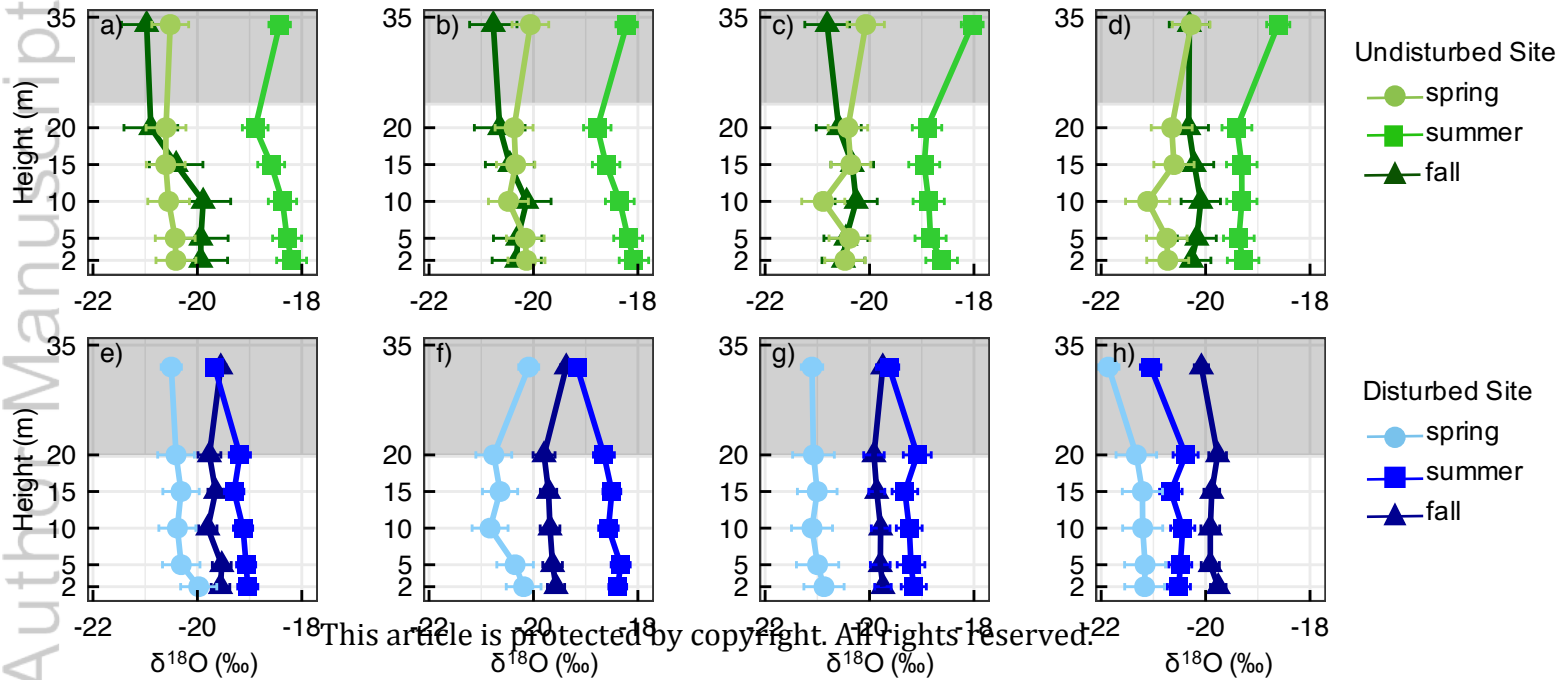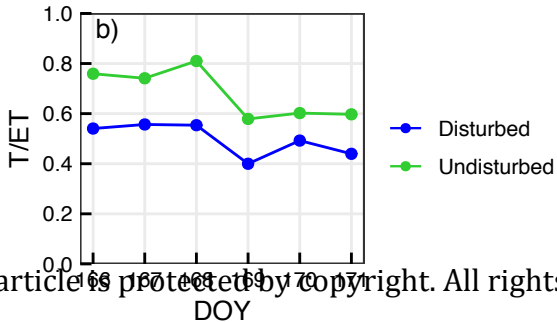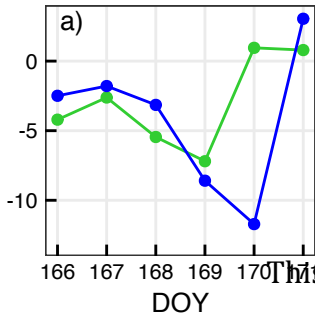
Legend: 2 m — 5 m — 10 m — 15 m — 20 m — 32/34 m

Spring · Summer · Fall

Legend: 2 m · 5 m · 10 m · 15 m · 20 m · 32/34 m

Undisturbed Site

p.m. ET/entrainment

a.m. ET

12 pm

6 pm

evening transpiration

early a.m. transpiration

6 am

GMWL

δD (‰)

-130

-135

-140

-145

-150

-21   -20   -19   -18   -17

Disturbed Site

p.m. ET/entrainment

12 pm

evening transpiration

a.m.

6 pm

GMWL

δD (‰)

-130

-135

-140

-145

-150

-21   -20   -19   -18   -17

$\delta^{18}O$ (‰)